Iran J Pharm Res. January-December 2024; 23(1): e157068 https://doi.org/10.5812/ijpr-157068

Published Online: 2025 January 5 **Research Article**

The Impact of Coenzyme Q10 on Cognitive Dysfunction, Antioxidant Defense, Cholinergic Activity, and Hippocampal Neuronal Damage in Monosodium Glutamate-Induced Obesity

Zahra Erfanmanesh [1], Mohammad Amin Edalatmanesh [1,*], Mokhtar Mokhtari [2]

[1] Department of Biology, Shiraz Branch, Islamic Azad University, Shiraz, Iran
[2] Department of Biology, Kazeroon Branch, Islamic Azad University, Kazeroon, Iran

[*] ***Corresponding Author:*** Department of Biology, Shiraz Branch, Islamic Azad University, Shiraz, Iran. Email: amin.edalatmanesh@gmail.com

Received: 21 October, 2024; **Revised:** 7 December, 2024; **Accepted:** 17 December, 2024

Abstract

Background: Obesity, a rising global health issue, is linked to numerous disorders, including cognitive impairment.

Objectives: This study investigates the effects of coenzyme Q10 (Co-Q10) on cognitive performance, antioxidant defense, cholinergic activity, and hippocampal neuron damage in rats rendered obese by monosodium glutamate (MSG) exposure.

Methods: Forty-eight neonatal male Wistar rats were randomly assigned to one of four groups: Control, MSG, MSG + Q10-10, and MSG + Q10-20. Monosodium glutamate (4 g/kg BW) was administered subcutaneously into the cervical region from postnatal day (PND) 2 to PND 10. Coenzyme Q10 (10 mg/kg BW and 20 mg/kg BW) was administered intraperitoneally from PND 30 to PND 42. At the end of the treatment period, working memory and avoidance learning tests were conducted. Anthropometric data were collected, followed by evaluations of hippocampal catalase (CAT), superoxide dismutase (SOD), acetylcholinesterase (AChE), glutathione peroxidase (GPx), and malondialdehyde (MDA) levels. The density of apoptotic/dark neurons (DN) in the CA_1 and CA_3 regions of the hippocampus was also assessed.

Results: Monosodium glutamate treatment increased Body Mass Index (BMI) and Lee Index, impaired working memory and avoidance learning, and reduced CAT, SOD, and GPx activities. Additionally, MSG exposure led to elevated MDA levels, increased AChE activity, and higher DN density in the CA_1 and CA_3 hippocampal regions. Treatment with Co-Q10 resulted in a decrease in BMI, enhanced memory and learning, noteworthy increases in CAT, SOD, and GPx activities in the hippocampus, and reductions in MDA levels, AChE activity, and DN density in the CA_1 and CA_3 regions.

Conclusions: Coenzyme Q10 mitigates hippocampal neuronal damage and improves cognitive function in MSG-induced obesity, primarily through its antioxidant and AChE inhibitory properties.

Keywords: Ubiquinone, Monosodium Glutamate, Hippocampus, Obesity, Rat

1. Background

The World Health Organization (WHO) classifies obesity as a global epidemic and one of the most noteworthy public health challenges today. According to WHO, obesity and overweight contribute to 2.8 million deaths annually, with global prevalence more than doubling since 1980 (1). Obesity noteworthyly elevates the risk of various cancers, respiratory diseases, arthritis, hypertension, dyslipidemia, cardiovascular disease, and type 2 diabetes (2). Furthermore, childhood obesity has been linked to a higher likelihood of developing cognitive disorders and dementia later in life (3).

Monosodium glutamate (MSG)-induced obesity, achieved through high-dose administration in the early postnatal period in rodents, leads to necrosis in hypothalamic structures, resulting in behavioral, cognitive, and motor dysfunction (4). Neonatal administration of MSG specifically destroys the ventromedial hypothalamic nucleus (VMH), leading to stunted growth and obesity (5).

Monosodium glutamate (E621) is a widely used flavor enhancer and legally approved food additive in many countries, particularly in Asia. Although its use is unrestricted in many regions, excessive consumption of MSG has toxic effects and increases the risk of obesity (6). In addition, MSG has been shown to cause structural brain changes, neurotoxicity, and oxidative stress (7). Overconsumption of MSG has been linked to neurodegenerative damage, Parkinson's disease (PD), epilepsy (E), and the stimulation of norepinephrine and dopamine release in various brain regions (8). Monosodium glutamate is particularly damaging to hypothalamic and hippocampal neurons, and neuronal damage and necrosis are monitored in several brain areas, including the hippocampus, following high doses of MSG due to increased glutamate levels (9).

The hippocampus plays a critical role in memory formation and behavioral regulation. Monosodium glutamate-induced damage to the hippocampus is associated with the formation of reactive oxygen species (ROS) and the impairment of antioxidant defenses. Since hippocampal intracellular and synaptic events continue to develop after birth, neonatal MSG exposure disrupts these critical processes (10).

The molecular mechanisms behind MSG-induced learning and memory impairments are thought to involve neurotransmitter imbalances and altered activity of enzymes such as acetylcholinesterase (AChE) and dopamine β-hydroxylase, which are involved in neurotransmitter metabolism (11). Research indicates that AChE is closely related to brain development, learning, memory, and neuronal damage. Increased AChE activity leads to rapid degradation of acetylcholine, resulting in diminished acetylcholine receptor stimulation and impaired cognitive function (12).

While many drugs previously used to manage obesity have been discontinued due to severe side effects, natural antioxidant compounds have gained acceptance as a safer therapeutic alternative (13). Coenzyme Q10 (Co-Q10), a fat-soluble benzoquinone found in all cells of the body, serves multiple functions despite its limited dietary availability (14). As an antioxidant, Co-Q10 prevents mitochondrial pore opening, protects cells from destruction, and exhibits anti-apoptotic properties (15). Brain levels of Co-Q10 decrease with age, making it a potential therapeutic agent for age-related neurodegenerative disorders (16). Coenzyme Q10 has been studied for its role in improving neurological disorders, including Alzheimer's disease AD, PD, depression (MDD), E, multiple sclerosis (MS), brain injuries (TBI), spinocerebellar ataxia (SCA), and Huntington's chorea (HD) (17).

2. Objectives

This study aims to investigate the effects of Co-Q10 on working and avoidance memory, oxidative stress markers, AChE activity, and apoptotic/dark neuron density in the hippocampus of MSG-induced obese rats.

3. Methods

3.1. Animal Treatment and Experimental Design

In this experimental study, 48 male neonatal Wistar rats were used. Twenty-five pregnant Wistar rats with known gestational day zero were obtained from the Razi Serum Institute and housed under standard conditions in the animal laboratory at Islamic Azad University, Shiraz. Each pregnant rat was housed individually in standard polycarbonate cages (manufactured by Razi Rad, Iran) under controlled conditions, with a temperature of 25 ± 1°C, 45 ± 5% relative humidity, and a 12/12-hour light/dark cycle (lights on at 7:00 AM). Standard rat chow and purified water were provided ad libitum. All experimental procedures followed international ethical guidelines and were approved by the Animal Ethics Committee of Islamic Azad University, Shiraz (ethics code: IR.IAU.SHIRAZ.REC.1399.009). Every effort was made to minimize animal use and reduce pain or discomfort. All dams delivered naturally, and neonate numbers and birth weights were recorded. The neonates stayed with their mothers until postnatal day (PND) 21, after which they were weaned and housed individually with standard food.

The neonates were randomly assigned (2 to 3 male offspring from each mother) to one of four groups (n = 12 per group): Control, MSG, MSG + Q10-10, and MSG + Q10-20. The control group received no treatment. In the MSG group, MSG (Sigma, Germany) was administered subcutaneously at a dose of 4 g/kg body weight from PND2 to PND10 in the cervical region (18). From PND30 to PND42, animals in this group received the Co-Q10 vehicle (sesame oil) intraperitoneally (I.P.) daily. In the MSG + Q10-10 and MSG + Q10-20 groups, in addition to MSG administration during the neonatal period, Co-Q10

(Sigma, Germany) was administered I.P. at doses of 10 mg/kg and 20 mg/kg body weight (19), respectively, from PND30 to PND42, along with the sesame oil vehicle. No mortality was monitored during the treatment period.

Anthropometric parameters, including naso-anal length and weight changes relative to birth weight, were measured on PND50. Body Mass Index (BMI) was calculated by dividing body weight (g) by the square of body length (cm^2), and the Lee Index, an indicator of obesity, was determined by dividing the cube root of body weight (g) by naso-anal length (cm) × 1000 (20).

3.2. Behavioral Tests Battery

3.2.1. Working Memory

At the end of the treatment period, on PND43, spatial working memory was assessed using the Y-maze for all groups (n = 12). The Y-maze consists of three identical arms, each measuring 15 ×30 × 40 cm, connected to a central area. At the start of the test, each animal was gently placed into one of the three arms without inducing stress, and its movements were monitored for 5 minutes. The number of entries into each arm was recorded, with an entry being defined as the placement of the animal's hind limb into an arm.

Alternation behavior, a measure of working memory, was defined as consecutive entries into all three arms in overlapping triplet sets. The percentage of alternation behavior, representing working memory performance, was calculated as the number of successful alternations divided by the total number of arm entries minus two, then multiplied by 100. A successful alternation was defined as three consecutive entries into all three arms in sequence (21).

3.2.2. Passive Avoidance Memory

On PND45, passive avoidance memory was evaluated in all groups (n = 12) using a shuttle box. The shuttle box consists of two compartments, one illuminated and one dark, with identical dimensions (27 × 14.5 × 14 cm) separated by a guillotine door. The floor of the dark compartment is equipped with steel rods (2 mm in diameter) connected to an electrical circuit. When activated, an electric current with specified duration, intensity, and frequency passes through the floor. The test is based on the natural tendency of rodents to avoid light and the aversive stimulus (electric shock) in the dark compartment. The test is divided into three main phases:

3.2.2.1. Habituation

Each animal was placed in the illuminated compartment for one minute to acclimate to the environment. After 30 seconds, the guillotine door was opened, allowing the animal to move freely into the dark compartment.

3.2.2.2. Acquisition

This phase took place 24 hours after habituation. The animal was placed in the illuminated compartment, and after 30 seconds, the guillotine door was opened, allowing it to enter the dark compartment. Upon entry, the guillotine door was closed, and an electric shock (2 mA, 2 seconds, 50 Hz) was delivered through the floor. The animal was removed 20 seconds after the shock and returned to its cage.

3.2.2.3. Retention

Retention tests were conducted 24 and 48 hours after the acquisition phase. During these tests, the animal was placed in the illuminated compartment, and after 30 seconds, the guillotine door was opened. The latency to enter the dark compartment (LDR) and the total time spent in the dark compartment (TDR) were recorded (22). No electric shocks were given during the retention tests. The cutoff time for the test was 300 seconds, and a longer delay in entering the dark compartment (LDR) was interpreted as successful memory retention.

3.3. Biochemical Studies

3.3.1. Oxidative Stress Parameters

On PND50, following the completion of behavioral tests, a subset of animals from each group (n = 8) was deeply anesthetized using a mixture of ketamine (50 mg/kg) and xylazine (5 mg/kg), after which the animals were immediately decapitated using a specialized rodent guillotine. The entire brain was rapidly removed and placed on ice. Under a stereoscope (Olympus, Japan), the hippocampus was carefully dissected from the brain. The tissue was washed with normal saline and Tris buffer (Sigma, Germany) and then homogenized using a homogenizer (IKA, Germany) for 10 minutes at 5000 rpm. The homogenized solution was subsequently

centrifuged in a refrigerated centrifuge (Hermle, Germany), and 0.5 mM phenylmethylsulfonyl fluoride (PMSF; Sigma-Aldrich, Germany) was added as a protease inhibitor (23). The supernatant obtained from the centrifugation process was used to assess oxidative stress markers.

Tissue levels of catalase (CAT), superoxide dismutase (SOD), and glutathione peroxidase (GPx) were measured using ELISA kits (Kia Zist, Iran) and an ELISA reader (Stat Fax, USA). Malondialdehyde (MDA) levels in the tissue were determined via spectrophotometry by measuring the reaction of MDA with thiobarbituric acid (Merck, Germany), with absorbance readings at 535 nm compared against a standard curve to quantify MDA concentration in the tissue samples.

3.3.2. Cholinergic Activity

Acetylcholinesterase activity in hippocampal tissue was measured via ACh hydrolysis using the Ellman method (24). A volume of 0.4 mL of the supernatant from hippocampal tissue homogenization was mixed with 2.6 mL of phosphate buffer (0.1 M, pH 7.4). Afterward, 0.1 mL of DTNB was added to the mixture, followed by 0.1 mL of acetylthiocholine iodide. Absorbance was measured at 412 nm with a spectrophotometer, and the change in absorbance was monitored over 2 minutes.

Acetylcholinesterase activity was determined by the increase in color resulting from the reaction between thiocholine and DTNB. The rate of absorbance change per minute was calculated, and AChE activity was expressed as micromoles of substrate hydrolyzed per minute per milligram of protein.

3.4. Histological Studies

To assess the density of dark neurons (DNs) in the hippocampus, a subset of animals from each group (n = 4) was anesthetized with a mixture of ketamine (50 mg/kg) and xylazine (5 mg/kg) on PND50, and immediate cardiac perfusion was performed. Following the fixation of brain tissue through cardiac perfusion, the brain was carefully removed from the skull and processed for histological studies using an autotechnicon. Parrafin blocks were prepared, and frontal sections of the hippocampus were made according to the Paxinos and Watson atlas. To assess the density of DNs, 1% toluidine blue staining was used (25). Imaging was performed using a light microscope (Olympus-BH2, Japan) with a 40x objective lens (total magnification of 400x).

After random sectioning, the density of DNs in the CA_1 and CA_3 regions of the hippocampus was measured using the disector method. Briefly, serial sections with a specified interval were prepared from the entire hippocampal region. In each section, cells were counted within a reference framework. The neuronal density was then calculated using the formula.

$$NA = \frac{\sum Q}{\sum P \times AH}$$

Where NA is the neuronal density, ∑Q is the total number of counted cells in a sample, ∑P is the number of sampling occurrences in a sample, A is the area of the sampling framework, and H is the distance between two consecutive sections or the thickness of each section (26). A minimum of 10 slides from each hippocampal sample (40 slides per group) were counted to evaluate the DN density.

3.5. Statistical Analysis

Statistical analysis of the data obtained from the various groups was conducted using SPSS software version 26. A one-way ANOVA followed by Tukey's post hoc test was performed to determine the presence of noteworthy divergences between the groups. Statistically noteworthy divergences were considered at $P < 0.05$.

4. Results

4.1. Changes in Body Weight, Body Length, Body Mass Index, and Lee Index

The study groups monitored Noteworthy divergences in body weight, BMI, and Lee Index (Table 1). A noteworthy increase in body weight was monitored in the MSG group in relation to the control group. The MSG group showed noteworthy increases in body weight ($P < 0.05$), BMI ($P < 0.01$), and Lee Index ($P < 0.05$) and a noteworthy decrease in body length ($P < 0.05$) in relation to the control group. In contrast, the groups receiving Co-Q10 showed no noteworthy divergences in the parameters in relation to the control group. In relation to the MSG group, the MSG + Q10-10 group showed a noteworthy increase in body length ($P < 0.05$)

Table 1. Mean ± Standard Deviation of Body Weight, Body Length, Body Mass Index, and Lee Index [a]

Parameters	Groups			
	Control	MSG	MSG + Q10-10	MSG + Q10-20
Body weight (g)	228.42 ± 19.6	260.09 ± 21.2 *	245.13 ± 15.4	232.36 ± 16.7 +
Body length (cm)	20.3 ± 0.9	19.1 ± 0.6 *	20.5 ± 0.8 +	20.0 ± 0.5 +
BMI (g/cm ^{2})	0.55 ± 0.05	0.71 ± 0.08 **	0.58 ± 0.07 ++	0.57 ± 0.07 ++
Lee's Index (g/cm)	0.30 ± 0.01	0.33 ± 0.01 *	0.31 ± 0.02	0.31 ± 0.01

Abbreviations: BMI, Body Mass Index; MSG, monosodium glutamate.

[a] Noteworthy divergences were monitored in the above parameters in relation to the control group (** P < 0.01, * P < 0.05). Furthermore, noteworthy divergences were monitored in some parameters between the MSG + Q10-10 and MSG + Q10-20 groups in relation to the MSG group (++ P < 0.01, + P < 0.05).

and a noteworthy decrease in BMI (P < 0.01). Moreover, the MSG + Q10-20 group exhibited a noteworthy reduction in body weight (P < 0.05) and BMI (P < 0.01) and a noteworthy increase in body length (P < 0.05) in relation to the MSG group.

4.2. Percentage of Alternation Behavior

Statistical analysis of alternation behavior percentage using one-way ANOVA and Tukey's post hoc test revealed noteworthy divergences among the study groups (Figure 1). Specifically, the percentage of alternation behavior (working memory) was noteworthyly reduced in the MSG and MSG + Q10-10 groups in relation to the control group (P < 0.001). However, the MSG + Q10-20 group showed a noteworthy increase in the percentage of alternation behavior in relation to the MSG group (P < 0.001). A noteworthy divergence was also monitored between the MSG + Q10-10 and MSG + Q10-20 groups (P < 0.01).

4.3. Passive Avoidance Memory

No noteworthy divergences in latency to enter the dark room (LDR) were monitored among the study groups during the acquisition phase (Figure 2). However, noteworthy divergences in LDR were noted at 24 and 48 hours after shock induction. At 24 hours post-shock, the MSG and MSG + Q10-10 groups exhibited a noteworthy decrease in LDR in relation to the control group (P < 0.001). Similarly, at 48 hours post-shock, both the MSG (P < 0.001) and MSG + Q10-10 (P < 0.01) groups showed a noteworthy reduction in LDR in relation to the control group. In contrast, the MSG + Q10-20 group demonstrated a noteworthy increase in LDR in relation to the MSG group at both 24 and 48 hours post-shock (P < 0.001). Additionally, the MSG + Q10-20 group showed a noteworthy increase in LDR in relation to the MSG + Q10-10 group at 24 hours post-shock (P < 0.05).

The mean time spent in the darkroom (TDR) during the acquisition phase showed no noteworthy divergences among the groups (Figure 3). However, noteworthy divergences in TDR were monitored at 24 and 48 hours after shock. At 24 hours post-shock, the MSG, MSG + Q10-10, and MSG + Q10-20 groups demonstrated a noteworthy increase in TDR in relation to the control group (P < 0.001). Similarly, at 48 hours post-shock, the MSG and MSG + Q10-10 (P < 0.001) groups showed a noteworthy increase in TDR in relation to the control group. Conversely, the MSG + Q10-20 group showed a noteworthy decrease in TDR in relation to the MSG group at both 24 and 48 hours post-shock (P < 0.001). A noteworthy divergence in TDR was also monitored between the MSG + Q10-10 and MSG + Q10-20 groups at 48 hours post-shock (P < 0.05).

During the acquisition phase, no noteworthy divergences were monitored in the TDR among the study groups (Figure 3). However, 24 and 48 hours after the shock, the TDR noteworthyly differed across the study groups. In relation to the control group, 24 hours after the shock, the MSG, MSG + Q10-10, and MSG + Q10-20 groups showed a noteworthy increase (P < 0.001). Additionally, 48 hours after the shock, the MSG and MSG + Q10-10 groups exhibited a noteworthy increase in relation to the control group (P < 0.001 and P < 0.01, respectively). In contrast, the MSG + Q10-20 group showed a noteworthy decrease in TDR in relation to the MSG group at 24 and 48 hours post-shock (P < 0.001). A noteworthy divergence was also monitored between the MSG + Q10-10 and MSG + Q10-20 groups 48 hours after the shock (P < 0.05).

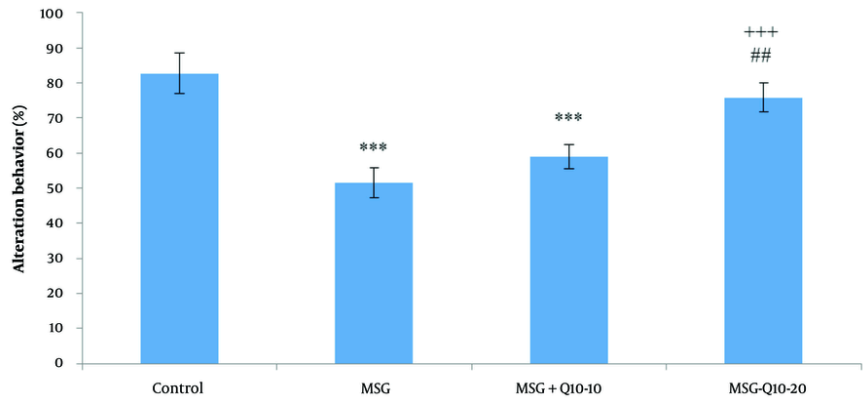

Figure 1. Comparison of mean ± standard deviation of the percentage of alternation behavior among the study groups. Noteworthy divergences were monitored between the control group and the monosodium glutamate (MSG) and MSG + Q10-10 groups (*** $P < 0.001$). In relation to the MSG group, the MSG + Q10-20 group showed a noteworthy increase (+++ $P < 0.001$). A noteworthy divergence was also monitored between the MSG + Q10-10 and MSG + Q10-20 groups (## $P < 0.01$).

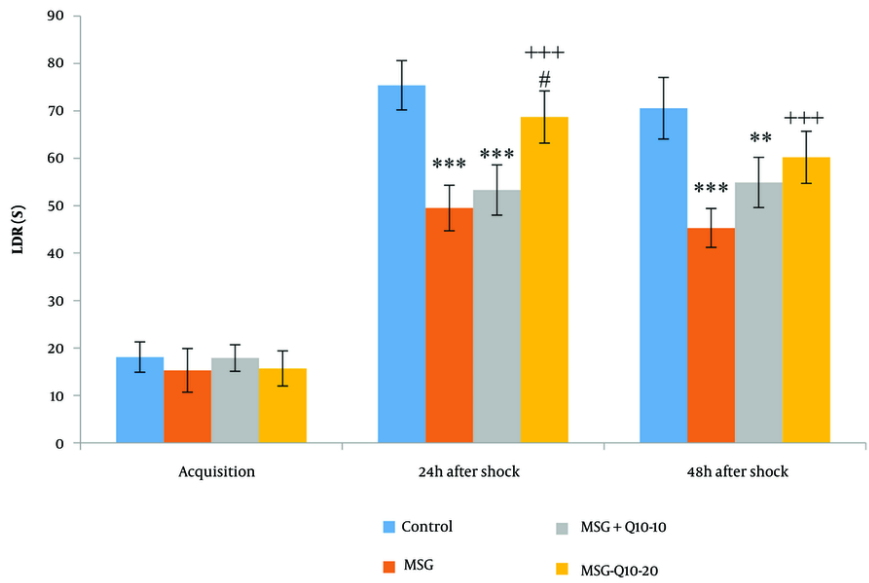

Figure 2. Comparison of mean ± standard deviation of LDR. During the acquisition phase, no noteworthy divergences were monitored between the groups. However, 24 and 48 hours post-shock, a noteworthy divergence was monitored between the control group and the monosodium glutamate (MSG) and MSG + Q10-10 groups (*** $P < 0.001$ and ** $P < 0.01$, respectively). In relation to the MSG group, the MSG + Q10-20 group showed a noteworthy increase at both time intervals after the shock (+++ $P < 0.001$). Furthermore, 24 hours after the shock, a noteworthy divergence was noted between the MSG + Q10-10 and MSG + Q10-20 groups (# $P < 0.05$).

4.4. Oxidative Stress Factors

The evaluation of CAT enzyme activity in the hippocampus showed noteworthy divergences among the study groups (Table 2). The MSG, MSG + Q10-10, and MSG + Q10-20 groups showed a noteworthy decrease in relation to the control group ($P < 0.001$). Furthermore, in relation to the MSG group, the MSG + Q10-10 and MSG

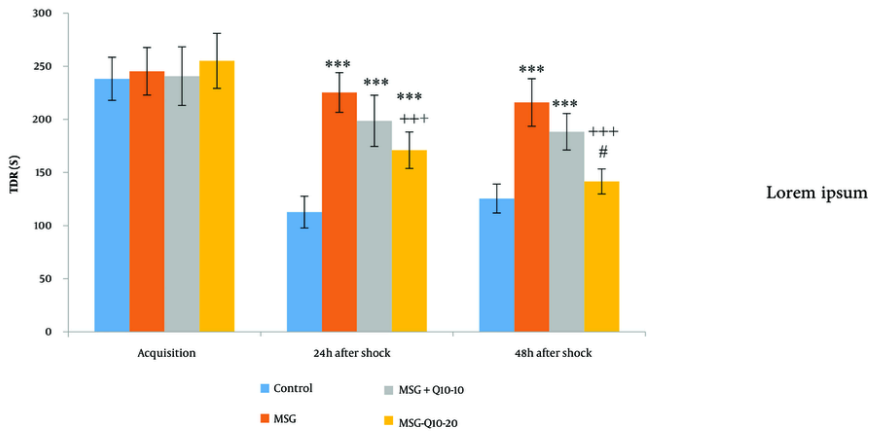

Figure 3. Comparison of mean ± standard deviation of TDR. No noteworthy divergences were monitored during the training phase among the study groups. However, in relation to the control group, noteworthy divergences were monitored in the MSG, MSG + Q10-10, and MSG + Q10-20 groups 24 hours post-shock and in the MSG and MSG + Q10-10 groups 48 hours post-shock (*** $P < 0.001$). The MSG + Q10-20 group showed a noteworthy decrease in TDR in relation to the MSG group at both time intervals post-shock (+++ $P < 0.001$). A noteworthy divergence was monitored between the MSG + Q10-10 and MSG + Q10-20 groups 48 hours after the shock (# $P < 0.05$).

Table 2. Mean ± Standard Deviation of Catalase, Superoxide dismutase, Glutathione Peroxidase Enzymatic Activities, and Monosodium Glutamate Content in the Hippocampus [a]

Groups	Parameters			
	CAT (mIU/mL)	SOD (pg/mL)	GPx (mIU/mL)	MDA (ng/mL)
Control	107.22 ± 7.6	73.49 ± 6.1	105.19 ± 6.1	32.07 ± 3.1
MSG	54.31 ± 6.5 ***	47.23 ± 4.8 ***	41.83 ± 4.7 ***	56.62 ± 4.7 ***
MSG + Q10-10	73.04 ± 6.9 ***, ++	52.31 ± 5.7 **	63.95 ± 6.5 ***, ++	48.31 ± 4.5 **
MSG + Q10-20	79.51 ± 5.4 ***, +++	67.82 ± 6.5 +++, #	91.70 ± 5.8 *, +++, ###	38.94 ± 3.7 +++, ##

Abbreviations: CAT, catalase; SOD, superoxide dismutase; GPx, glutathione peroxidase; MDA, malondialdehyde; MSG, monosodium glutamate

[a] In relation to the control group, the MSG, MSG + Q10-10, and MSG + Q10-20 groups showed noteworthy divergences in the above parameters (*** $P < 0.001$, ** $P < 0.01$, and * $P < 0.05$). Additionally, in relation to the MSG group, noteworthy divergences were monitored in the MSG + Q10-10 and MSG + Q10-20 groups (+++ $P < 0.001$ and ++ $P < 0.01$). Moreover, a noteworthy divergence was monitored between the MSG + Q10-10 and MSG + Q10-20 groups (### $P < 0.001$, ## $P < 0.01$, and # $P < 0.05$).

+ Q10-20 groups exhibited a noteworthy increase ($P < 0.01$ and $P < 0.001$, respectively).

The analysis of hippocampal SOD activity also revealed noteworthy divergences among the study groups (Table 2). Superoxide dismutase activity in the MSG and MSG + Q10-10 groups was noteworthyly decreased in relation to the control group ($P < 0.01$ and $P < 0.001$, respectively). Conversely, the MSG + Q10-20 group showed a noteworthy increase in SOD activity in relation to the MSG group ($P < 0.001$). Moreover, a noteworthy divergence was monitored between the MSG + Q10-10 and MSG + Q10-20 groups ($P < 0.05$).

Hippocampal GPx levels also noteworthyly differed across the groups (Table 2). In relation to the control group, the MSG, MSG + Q10-10, and MSG + Q10-20 groups showed a noteworthy decrease ($P < 0.001$, $P < 0.001$, and $P < 0.05$, respectively). In relation to the MSG group, the MSG + Q10-10 and MSG + Q10-20 groups have demonstrated a noteworthy increase ($P < 0.01$ and $P < 0.001$, respectively). Furthermore, a noteworthy divergence was monitored between the MSG + Q10-10 and MSG + Q10-20 groups ($P < 0.001$).

The analysis of hippocampal MDA content indicated noteworthy divergences among the study groups (Table 2). Specifically, a noteworthy increase was monitored in the MSG and MSG + Q10-10 groups in relation to the control group ($P < 0.001$ and $P < 0.01$, respectively). In relation to the MSG group, the MSG + Q10-20 group

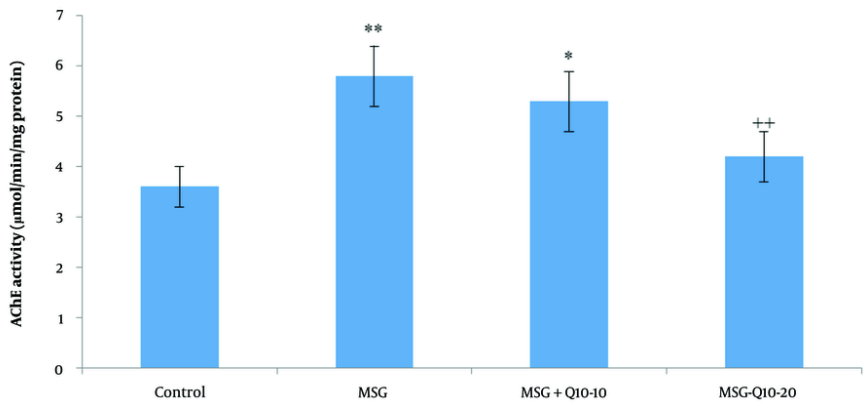

Figure 4. Comparison of mean ± standard deviation of hippocampal acetylcholinesterase (AChE) activity across study groups. The results indicate a noteworthy divergence between the control group and the monosodium glutamate (MSG) and MSG + Q10-10 groups (** $P < 0.01$ and * $P < 0.05$, respectively). The MSG + Q10-20 group demonstrated a noteworthy decrease in AChE activity in relation to the MSG group (++ $P < 0.01$).

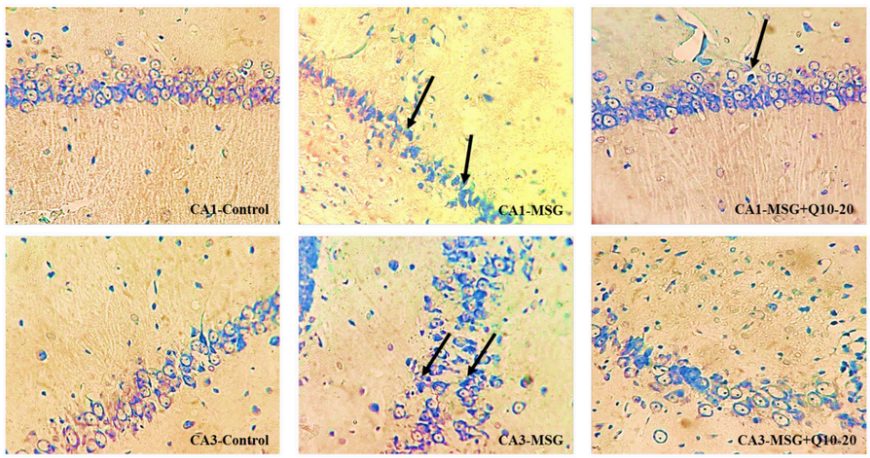

Figure 5. Photomicrographs of the CA_1 and CA_3 regions of the hippocampus across study groups. An increased density of dark neurons (DNs) is monitored in the monosodium glutamate (MSG) group in relation to the control group. Conversely, a lower density of DNs is noticeable in the MSG + Q10-20 group. Toluidine blue staining. Black arrows indicate DN. Magnification: 40X.

exhibited a noteworthy decrease ($P < 0.001$). A noteworthy divergence was also monitored between the MSG + Q10-10 and MSG + Q 10 - 20 groups ($P < 0.01$).

4.5. Cholinergic Activity

The data analysis revealed a noteworthy divergence in hippocampal AChE activity among the study groups (Figure 4). Acetylcholinesterase activity in the MSG and MSG + Q10-10 groups was noteworthyly increased in relation to the control group ($P < 0.01$ and $P < 0.05$, respectively). Additionally, in relation to the MSG group, the MSG + Q10-20 group showed a noteworthy decrease in hippocampal AChE activity ($P < 0.01$).

4.6. Density of DNs

DNs were monitored in various brain regions using Toluidine Blue Staining. This study examined the density of DNs in the CA_1 and CA_3 regions of the hippocampus

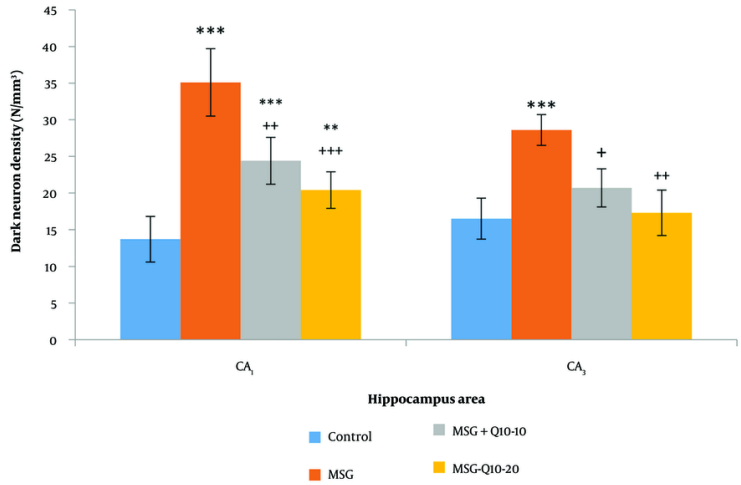

Figure 6. Comparison of mean ± standard deviation of dark neurons (DN) density in the and CA_3 regions of the hippocampus across different groups. Noteworthy divergences were monitored between the control group and the monosodium glutamate (MSG), MSG + Q10-10, and MSG + Q10-20 groups in the region and with the MSG group in the CA_3 region (*** $P < 0.001$ and ** $P < 0.01$, respectively). Additionally, in relation to the MSG group, the MSG + Q10-10 and MSG + Q10-20 groups demonstrated a noteworthy decrease in dark neuron density in both regions (+++ $P < 0.001$, ++ $P < 0.01$, and + $P < 0.05$, respectively).

across different groups (Figure 5). The data analysis showed a noteworthy divergence between the control and MSG groups in the CA_1 and CA_3 regions ($P < 0.001$). In the CA_1 region, the MSG + Q10-10 and MSG + Q10-20 groups showed a noteworthy increase in dark neuron density in relation to the control group ($P < 0.001$ and $P < 0.01$, respectively). In relation to the MSG group, the MSG + Q10-10 and MSG + Q10-20 groups exhibited a noteworthy decrease in dark neuron density in the CA_1 region ($P < 0.01$ and $P < 0.001$, respectively) and in the CA_3 region ($P < 0.05$ and $P < 0.01$, respectively) (Figure 6).

5. Discussion

Obesity is regarded as the most prevalent health issue and nutritional disorder in developed countries (2). Monosodium glutamate is a naturally occurring non-essential amino acid, but excessive consumption can lead to substantial metabolic alterations and severe bodily disorders (27). In neonatal rats, MSG treatment causes hypothalamic lesions, disrupting feeding behavior, increasing food intake, and elevating blood glucose levels (28). Additionally, MSG disrupts brain functions and induces oxidative stress, which may result in sudden neuronal death, acute degenerative changes, and chronic neurological defects (29).

This study found noteworthy increases in body weight, BMI, and Lee Index in the MSG-treated group in relation to controls. Neonatal MSG administration, as a model of obesity, damaged the hippocampus and led to the formation of neuronal artifacts during adolescence (PND50), visible as DNs in toluidine blue staining. The density of DNs in various hippocampal regions was noteworthyly higher in the MSG group than in the control group. Additionally, oxidative damage in the hippocampus was characterized by reduced activity of antioxidant enzymes (CAT, SOD, and GPx) and increased lipid peroxidation in MSG-treated rats. Notably, hippocampal AChE activity was noteworthyly elevated in the MSG group in relation to controls. However, treatment with Co-Q10 improved hippocampal antioxidant activity, inhibited AChE, and noteworthyly reduced DN density in various hippocampal subareas, preventing MSG-induced memory and learning impairments.

Glutamate crosses the BBB in limited quantities through active transport, which is tightly regulated to protect the brain from excitotoxicity. However, because the BBB is underdeveloped at birth, MSG can more easily

penetrate the brain, reducing arcuate nucleus activity and neurons in the satiety center. As a result, neonatal MSG-treated rats often exhibit hyperphagia and obesity (30). Following MSG treatment, brain plasma glutamate concentrations rise substantially above normal levels, leading to excessive glutamate receptor activation and resulting in apoptosis and necrosis of neuronal cells (31). This overactivation releases calcium ions from intracellular stores and maximally activates mitochondria, as well as endonucleases, phospholipases, and proteases, which destroy cellular structures, plasma membranes, and DNA (32).

The hippocampus, a region particularly vulnerable to oxidative stress and glutamate-induced excitotoxicity, plays a crucial role in spatial learning and memory (33). Memory impairments associated with hippocampal dysfunction (working-spatial memory) monitored in the MSG group in this study may be due to alterations in glutamate neurotransmission and changes in glutamate receptor expression. Research has shown that loss of NMDA glutamate receptors in the hippocampus can impair learning (34). Furthermore, increased glutamate accumulation in the hippocampus has been linked to damage in CA_1 pyramidal neurons, as monitored in this study (35).

Acetylcholine is a critical neurotransmitter in the brain, and disruptions in its storage, release, and metabolism are associated with behavioral, cognitive, learning, and memory disorders, as well as neurodegenerative diseases (36). This study demonstrated that neonatal MSG administration increased hippocampal AChE activity. Increased AChE activity accelerates acetylcholine metabolism in the synaptic cleft and reduces cholinergic neurotransmission efficiency, causing progressive cognitive impairments (36). Furthermore, previous studies indicate that MSG induces oxidative stress by increasing lipid peroxides and ROS, which may further elevate AChE activity (37). In contrast, other research has found that L-glutamate administration decreased AChE activity (38). However, the dose used in those studies (103 mg/kg) was much lower than the acute dose (4 g/kg) used in the present study, and it was administered during adulthood rather than the neonatal period. In this study, Co-Q10 at 20 mg/kg inhibited AChE activity. Given that AChE inhibitors are the first-line treatment for cognitive disorders, dementia, and AD, Co-Q10, which has minimal side effects, could be a promising alternative to traditional drugs that are associated with undesirable side effects such as nausea, diarrhea, and appetite loss (39). Kumar et al. demonstrated that Co-Q10 improves cognitive functions and reduces AChE activity in AD models in adult rats (40).

Hippocampal oxidative stress, as indicated by increased lipid peroxidation and decreased activity of CAT, SOD, and GPx, is one of the toxic effects of MSG. Oxidative stress is a hallmark of neurological diseases. Despite the brain's high metabolic activity, it has limited antioxidant capacity. The production of free radicals leads to lipid peroxidation and oxidative DNA damage, resulting in cellular damage and apoptosis (41). Oxidative stress also disrupts BBB function, stimulates glutamate receptors, and activates inflammatory and apoptotic signaling pathways (42).

Conversely, this study demonstrated that Co-Q10 possesses potent antioxidant properties, improving working and avoidance memory in MSG-induced obese rat models. Coenzyme Q10 is most concentrated in tissues with high energy demands, such as the brain. It plays a vital role in cellular processes, including regulating cellular metabolism, oxidative stress, H_2O_2 formation, bioenergetics, and gene regulation (43). Coenzyme Q10 enhances mitochondrial function in neurons by increasing ATP synthesis and has demonstrated neuroprotective effects in various neurological and psychiatric disorders, including AD, PD, and MDD (44). Following neonatal MSG treatment, this study monitored an increased density of DNs in various hippocampal subareas. Rapid glutamate release can induce DN formation in the brain (45), which persists into adolescence. Dark neurons are dying or degenerating neurons characterized by a hyperbasophilic appearance and highly condensed ultrastructure. Dark neurons prevalence has been monitored in the CA_1, amygdala, cortical pyramidal layer, and other limbic structures in various brain injury models, as evidenced by cresyl violet or toluidine blue staining (46). Our study showed that the effects of MSG on CA_1 and CA_2 vulnerability are different. Although recent studies on the selective vulnerability of CA_1 to CA_3 neurons have shown conflicting results, and depending on several factors, such as the method and animal model, the vulnerability of different hippocampal subfields will vary. However, considering possible mechanisms (intrinsic oxidative stress potential and

mitochondrial dysregulation) in CA_1 and CA_2 can explain this differential vulnerability (35).

5.1. Conclusions

The MSG-induced obesity model resulted in noteworthy damage to the hippocampus of rats, characterized by a high density of DNs. Reduced hippocampal antioxidant capacity and increased AChE activity also impaired working and avoidance memory. Furthermore, Co-Q10 noteworthyly ameliorated hippocampal cellular damage, reduced the density of DNs, and, through its antioxidant effects and AChE inhibitory action, improved memory and learning in the pathology induced by neonatal MSG consumption. Treatment with Co-Q10 offers a promising potential for the prevention and treatment of complications associated with MSG toxicity. At the end, we recommended the investigation of long-term effects of Co-Q10 on cognitive function, exploration of the potential gender differences, examination of the molecular pathways, particularly its impact on glutamate receptors and synaptic plasticity, evaluation of the efficacy Co-Q10 in combination with other antioxidant compounds for synergistic effects in preventing MSG-induced cognitive impairments and conduction of clinical trials to determine the applicability of Co-Q10 in preventing and treating cognitive impairments in humans exposed to high MSG levels.

Footnotes

Authors' Contribution: Z. E.: Investigation, formal analysis, and writing-original draft preparation; M. A. E.: Supervision, conceptualization, methodology, data curation, formal analysis, writing-review and editing; M. M.: Methodology, writing- review and editing.

Conflict of Interests Statement: The authors have declared that there is no conflict of interest.

Data Availability: The dataset presented in the study is available on request from the corresponding author during submission or after publication. The data are not publicly available because the data of this study are taken from the Ph.D. thesis of the first author. The authors are advised not to send the data at this stage, if any of the referees or editors request to send specific data, the data will be sent.

Ethical Approval: Ethical principles, in accordance with international guidelines and the Animal Ethics Committee of Islamic Azad University, Shiraz Branch (ethics code: IR.IAU.SHIRAZ.REC.1399.009), were strictly followed.

Funding/Support: This work was partially supported by Islamic Azad University, Shiraz Branch, Shiraz, Iran.

References

1. Hernandez Bautista RJ, Mahmoud AM, Konigsberg M, Lopez Diaz Guerrero NE. Obesity: Pathophysiology, monosodium glutamate-induced model and anti-obesity medicinal plants. *Biomed Pharmacother*. 2019;**111**:503-16. [PubMed ID: 30597304]. https://doi.org/10.1016/j.biopha.2018.12.108.
2. Lin X, Li H. Obesity: Epidemiology, Pathophysiology, and Therapeutics. *Front Endocrinol (Lausanne)*. 2021;**12**:706978. [PubMed ID: 34552557]. [PubMed Central ID: PMC8450866]. https://doi.org/10.3389/fendo.2021.706978.
3. Marti-Nicolovius M. [Effects of overweight and obesity on cognitive functions of children and adolescents]. *Rev Neurol*. 2022;**75**(3):59-65. ES. [PubMed ID: 35879881]. [PubMed Central ID: PMC10280776]. https://doi.org/10.33588/rn.7503.2022173.
4. de Andrade BZ, Zazula MF, Bittencourt Guimaraes AT, Sagae Schneider SC, Boaretto ML, Felicio Poncio AC, et al. Whole-body vibration promotes lipid mobilization in hypothalamic obesity rat. *Tissue Cell*. 2021;**68**:101456. [PubMed ID: 33202347]. https://doi.org/10.1016/j.tice.2020.101456.
5. Muraro EN, Sbardelotto BM, Guareschi ZM, de Almeida W, Souza Dos Santos A, Grassiolli S, et al. Vitamin D supplementation combined with aerobic physical exercise restores the cell density in hypothalamic nuclei of rats exposed to monosodium glutamate. *Clin Nutr ESPEN*. 2022;**52**:20-7. [PubMed ID: 36513455]. https://doi.org/10.1016/j.clnesp.2022.09.009.
6. Chakraborty SP. Patho-physiological and toxicological aspects of monosodium glutamate. *Toxicol Mech Methods*. 2019;**29**(6):389-96. [PubMed ID: 30273089]. https://doi.org/10.1080/15376516.2018.1528649.
7. Kumar M, Kumar A, Sindhu RK, Kushwah AS. Arbutin attenuates monosodium L-glutamate induced neurotoxicity and cognitive dysfunction in rats. *Neurochem Int*. 2021;**151**:105217. [PubMed ID: 34710534]. https://doi.org/10.1016/j.neuint.2021.105217.
8. Pisano CA, Brugnoli A, Novello S, Caccia C, Keywood C, Melloni E, et al. Safinamide inhibits in vivo glutamate release in a rat model of Parkinson's disease. *Neuropharmacol J*. 2020;**167**:108006. [PubMed ID: 32086070]. https://doi.org/10.1016/j.neuropharm.2020.108006.
9. Yousof SM, Awad YM, Mostafa EMA, Hosny MM, Anwar MM, Eldesouki RE, et al. The potential neuroprotective role of Amphora coffeaeformis algae against monosodium glutamate-induced neurotoxicity in adult albino rats. *Food Funct*. 2021;**12**(2):706-16. [PubMed ID: 33337454]. https://doi.org/10.1039/d0fo01957g.

10. Helal AM, Abdel-Latif MS, Abomughaid MM, Ghareeb DA, El-Sayed MM. Potential therapeutic effects of Ulva lactuca water fraction on monosodium glutamate-induced testicular and prostatic tissue damage in rats. *Environ Sci Pollut Res Int*. 2021;**28**(23):29629-42. [PubMed ID: 33559824]. https://doi.org/10.1007/s11356-021-12387-x.
11. Khalil RM, Khedr NF. Curcumin Protects against Monosodium Glutamate Neurotoxicity and Decreasing NMDA2B and mGluR5 Expression in Rat Hippocampus. *Neurosignals*. 2016;**24**(1):81-7. [PubMed ID: 27529496]. https://doi.org/10.1159/000442614.
12. Walczak-Nowicka LJ, Herbet M. Acetylcholinesterase Inhibitors in the Treatment of Neurodegenerative Diseases and the Role of Acetylcholinesterase in their Pathogenesis. *Int J Mol Sci*. 2021;**22**(17). [PubMed ID: 34502198]. [PubMed Central ID: PMC8430571]. https://doi.org/10.3390/ijms22179290.
13. Shaik Mohamed Sayed UF, Moshawih S, Goh HP, Kifli N, Gupta G, Singh SK, et al. Natural products as novel anti-obesity agents: insights into mechanisms of action and potential for therapeutic management. *Front Pharmacol*. 2023;**14**:1182937. [PubMed ID: 37408757]. [PubMed Central ID: PMC10318930]. https://doi.org/10.3389/fphar.2023.1182937.
14. Pravst I, Rodriguez Aguilera JC, Cortes Rodriguez AB, Jazbar J, Locatelli I, Hristov H, et al. Comparative Bioavailability of Different Coenzyme Q10 Formulations in Healthy Elderly Individuals. *Nutr J*. 2020;**12**(3). [PubMed ID: 32188111]. [PubMed Central ID: PMC7146408]. https://doi.org/10.3390/nu12030784.
15. Hidalgo-Gutierrez A, Gonzalez-Garcia P, Diaz-Casado ME, Barriocanal-Casado E, Lopez-Herrador S, Quinzii CM, et al. Metabolic Targets of Coenzyme Q10 in Mitochondria. *Antioxidant J (Basel)*. 2021;**10**(4). [PubMed ID: 33810539]. [PubMed Central ID: PMC8066821]. https://doi.org/10.3390/antiox10040520.
16. Bagheri S, Haddadi R, Saki S, Kourosh-Arami M, Rashno M, Mojaver A, et al. Neuroprotective effects of coenzyme Q10 on neurological diseases: a review article. *Front Neurosci*. 2023;**17**:1188839. [PubMed ID: 37424991]. [PubMed Central ID: PMC10326389]. https://doi.org/10.3389/fnins.2023.1188839.
17. Kadian M, Sharma G, Pandita S, Sharma K, Shrivasatava K, Saini N, et al. The Impact of Coenzyme Q10 on Neurodegeneration: a Comprehensive Review. *Curr Pharmacol Rep*. 2022;**8**(1):1-19. https://doi.org/10.1007/s40495-021-00273-6.
18. Seiva FR, Chuffa LG, Braga CP, Amorim JP, Fernandes AA. Quercetin ameliorates glucose and lipid metabolism and improves antioxidant status in postnatally monosodium glutamate-induced metabolic alterations. *Food Chem Toxicol*. 2012;**50**(10):3556-61. [PubMed ID: 22809473]. https://doi.org/10.1016/j.fct.2012.07.009.
19. Gholipour F, Shams J, Zahiroddin A. Protective Effect of Coenzyme Q10 on Methamphetamine-Induced Apoptosis in Adult Male Rats. *Novelty Biomed*. 2017;**5**(3):127-32. https://doi.org/10.22037/nbm.v5i3.17397.
20. Nabi S, Bhandari U, Haque SE. Saroglitazar ameliorates monosodium glutamate-induced obesity and associated inflammation in Wistar rats: Plausible role of NLRP3 inflammasome and NF- kappaB. *Iran J Basic Med Sci*. 2022;**25**(7):827-41. [PubMed ID: 36033946]. [PubMed Central ID: PMC9392566]. https://doi.org/10.22038/IJBMS.2022.64041.14102.
21. Safarpour M, Edalatmanesh MA, Hossini SE, Forouzanfar M. [Neuroprotective Effect of Cinnamic Acid on Cognitive Impairment and the Level of Oxidative Stress Indicators in Rat's Offspring in an Uteroplacental Insufficiency Model]. *J Ilam Univ Med Sci*. 2021;**28**(6):33-46. FA. https://doi.org/10.29252/sjimu.28.6.33.
22. Vafaee F, Hosseini M, Hassanzadeh Z, Edalatmanesh MA, Sadeghnia HR, Seghatoleslam M, et al. The Effects of Nigella Sativa Hydro-alcoholic Extract on Memory and Brain Tissues Oxidative Damage after Repeated Seizures in Rats. *Iran J Pharm Res*. 2015;**14**(2):547-57. [PubMed ID: 25901163]. [PubMed Central ID: PMC4403072].
23. Abdollahi H, Edalatmanesh MA, Hosseini E, Foroozanfar M. The Effects of Hesperidin on BDNF/TrkB Signaling Pathway and Oxidative Stress Parameters in the Cerebral Cortex of the Utero-placental Insufficiency Fetal Rat Model. *Basic Clin Neurosci*. 2021;**12**(4):511-22. [PubMed ID: 35154591]. [PubMed Central ID: PMC8817181]. https://doi.org/10.32598/bcn.2021.2187.1.
24. Wopara I, Modo EU, Adebayo OG, Mobisson SK, Nwigwe JO, Ogbu PI, et al. Anxiogenic and memory impairment effect of food color exposure: upregulation of oxido-neuroinflammatory markers and acetyl-cholinestrase activity in the prefrontal cortex and hippocampus. *Heliyon J*. 2021;**7**(3). e06378. [PubMed ID: 33748463]. [PubMed Central ID: PMC7970276]. https://doi.org/10.1016/j.heliyon.2021.e06378.
25. Pourzaki M, Homayoun M, Sadeghi S, seghatoleslam M, Hosseini M, Ebrahimzadeh Bideskan A. Preventive effect of Coriandrum sativum on neuronal damages in pentylentetrazole-induced seizure in rats. *Avicenna J Phytomed*. 2017;**7**(2):116-28. https://doi.org/10.22038/ajp.2016.7757.
26. Bagheri-Abassi F, Alavi H, Mohammadipour A, Motejaded F, Ebrahimzadeh-Bideskan A. The effect of silver nanoparticles on apoptosis and dark neuron production in rat hippocampus. *Iran J Basic Med Sci*. 2015;**18**(7):644-8. [PubMed ID: 26351553]. [PubMed Central ID: PMC4556755].
27. Kayode OT, Bello JA, Oguntola JA, Kayode AAA, Olukoya DK. The interplay between monosodium glutamate (MSG) consumption and metabolic disorders. *Heliyon*. 2023;**9**(9). e19675. [PubMed ID: 37809920]. [PubMed Central ID: PMC10558944]. https://doi.org/10.1016/j.heliyon.2023.e19675.
28. Zanfirescu A, Ungurianu A, Tsatsakis AM, Nitulescu GM, Kouretas D, Veskoukis A, et al. A review of the alleged health hazards of monosodium glutamate. *Compr Rev Food Sci Food Saf*. 2019;**18**(4):1111-34. [PubMed ID: 31920467]. [PubMed Central ID: PMC6952072]. https://doi.org/10.1111/1541-4337.12448.
29. Feng J, Zheng Y, Guo M, Ares I, Martinez M, Lopez-Torres B, et al. Oxidative stress, the blood-brain barrier and neurodegenerative diseases: The critical beneficial role of dietary antioxidants. *Acta Pharm Sin B*. 2023;**13**(10):3988-4024. [PubMed ID: 37799389]. [PubMed Central ID: PMC10547923]. https://doi.org/10.1016/j.apsb.2023.07.010.
30. Nakadate K, Kawakami K, Yamazaki N. Anti-Obesity and Anti-Inflammatory Synergistic Effects of Green Tea Catechins and Citrus beta-Cryptoxanthin Ingestion in Obese Mice. *Int J Mol Sci*. 2023;**24**(8). [PubMed ID: 37108217]. [PubMed Central ID: PMC10138730]. https://doi.org/10.3390/ijms24087054.
31. Wang J, Wang F, Mai D, Qu S. Molecular Mechanisms of Glutamate Toxicity in Parkinson's Disease. *Front Neurosci*. 2020;**14**:585584. [PubMed ID: 33324150]. [PubMed Central ID: PMC7725716]. https://doi.org/10.3389/fnins.2020.585584.
32. Matuz-Mares D, Gonzalez-Andrade M, Araiza-Villanueva MG, Vilchis-Landeros MM, Vazquez-Meza H. Mitochondrial Calcium: Effects of Its Imbalance in Disease. *Antioxidant J (Basel)*. 2022;**11**(5). [PubMed ID: 35624667]. [PubMed Central ID: PMC9138001]. https://doi.org/10.3390/antiox11050801.
33. Keimasi M, Salehifard K, Keimasi M, Amirsadri M, Esfahani NMJ, Moradmand M, et al. Corrigendum: Alleviation of cognitive deficits

in a rat model of glutamate-induced excitotoxicity, using an N-type voltage-gated calcium channel ligand, extracted from Agelena labyrinthica crude venom. *Front Mol Neurosci*. 2023;**16**:1180964. [PubMed ID: 37008777]. [PubMed Central ID: PMC10061123]. https://doi.org/10.3389/fnmol.2023.1180964.

34. Tsai YC, Huang SM, Peng HH, Lin SW, Lin SR, Chin TY, et al. Imbalance of synaptic and extrasynaptic NMDA receptors induced by the deletion of CRMP1 accelerates age-related cognitive decline in mice. *Neurobiol Aging*. 2024;**135**:48-59. [PubMed ID: 38176125]. https://doi.org/10.1016/j.neurobiolaging.2023.12.006.
35. Einenkel AM, Salameh A. Selective vulnerability of hippocampal CA1 and CA3 pyramidal cells: What are possible pathomechanisms and should more attention be paid to the CA3 region in future studies? *J Neurosci Res*. 2024;**102**(1). e25276. [PubMed ID: 38284845]. https://doi.org/10.1002/jnr.25276.
36. Liang Q, Li D, Li J, Li Y, Zou Y, Zhang Y. Protective effect of Danshensu against neurotoxicity induced by monosodium glutamate in adult mice and their offspring. *Heliyon J*. 2024;**10**(3). e25546. [PubMed ID: 38356496]. [PubMed Central ID: PMC10865244]. https://doi.org/10.1016/j.heliyon.2024.e25546.
37. Abu-Taweel GM, A ZM, Ajarem JS, Ahmad M. Cognitive and biochemical effects of monosodium glutamate and aspartame, administered individually and in combination in male albino mice. *Neurotoxicol Teratol*. 2014;**42**:60-7. [PubMed ID: 24556450]. https://doi.org/10.1016/j.ntt.2014.02.001.
38. Tabassum S, Ahmad S, Madiha S, Shahzad S, Batool Z, Sadir S, et al. Free L-glutamate-induced modulation in oxidative and neurochemical profile contributes to enhancement in locomotor and memory performance in male rats. *Sci Rep*. 2020;**10**(1):11206. [PubMed ID: 32641780]. [PubMed Central ID: PMC7343824]. https://doi.org/10.1038/s41598-020-68041-y.
39. Moreira N, Lima J, Marchiori MF, Carvalho I, Sakamoto-Hojo ET. Neuroprotective Effects of Cholinesterase Inhibitors: Current Scenario in Therapies for Alzheimer's Disease and Future Perspectives. *J Alzheimers Dis Rep*. 2022;**6**(1):177-93. [PubMed ID: 35591949]. [PubMed Central ID: PMC9108627]. https://doi.org/10.3233/ADR-210061.
40. Kumar P, Singh A, Kumar A, Kumar R, Pal R, Sachan AK, et al. Effect of Curcumin and Coenzyme Q10 Alone and in Combination on Learning and Memory in an Animal Model of Alzheimer's Disease. *Biomed J*. 2023;**11**(5). [PubMed ID: 37239093]. [PubMed Central ID: PMC10216191]. https://doi.org/10.3390/biomedicines11051422.
41. Olufunmilayo EO, Gerke-Duncan MB, Holsinger RMD. Oxidative Stress and Antioxidants in Neurodegenerative Disorders. *Antioxidant J (Basel)*. 2023;**12**(2). [PubMed ID: 36830075]. [PubMed Central ID: PMC9952099]. https://doi.org/10.3390/antiox12020517.
42. Kim Y, Cho AY, Kim HC, Ryu D, Jo SA, Jung YS. Effects of Natural Polyphenols on Oxidative Stress-Mediated Blood-Brain Barrier Dysfunction. *Antioxidant J (Basel)*. 2022;**11**(2). [PubMed ID: 35204080]. [PubMed Central ID: PMC8868362]. https://doi.org/10.3390/antiox11020197.
43. Suarez-Rivero JM, Pastor-Maldonado CJ, Povea-Cabello S, Alvarez-Cordoba M, Villalon-Garcia I, Munuera-Cabeza M, et al. Coenzyme Q(10) Analogues: Benefits and Challenges for Therapeutics. *Antioxidant J (Basel)*. 2021;**10**(2). [PubMed ID: 33557229]. [PubMed Central ID: PMC7913973]. https://doi.org/10.3390/antiox10020236.
44. Ebrahimi A, Kamyab A, Hosseini S, Ebrahimi S, Ashkani-Esfahani S. Involvement of Coenzyme Q10 in Various Neurodegenerative and Psychiatric Diseases. *Biochem Res Int*. 2023;**2023**:5510874. [PubMed ID: 37946741]. [PubMed Central ID: PMC10632062]. https://doi.org/10.1155/2023/5510874.
45. Nicosia N, Giovenzana M, Misztak P, Mingardi J, Musazzi L. Glutamate-Mediated Excitotoxicity in the Pathogenesis and Treatment of Neurodevelopmental and Adult Mental Disorders. *Int J Mol Sci*. 2024;**25**(12). [PubMed ID: 38928227]. [PubMed Central ID: PMC11203689]. https://doi.org/10.3390/ijms25126521.
46. Zsombok A, Toth Z, Gallyas F. Basophilia, acidophilia and argyrophilia of "dark" (compacted) neurons during their formation, recovery or death in an otherwise undamaged environment. *J Neurosci Methods*. 2005;**142**(1):145-52. [PubMed ID: 15652628]. https://doi.org/10.1016/j.jneumeth.2004.08.005.